Rare Metal Materials and Engineering
Volume 55, Issue 3, March 2026
Available online at www.rmme.ac.cn

Science Press

Cite this article as: Wang Rui, Li Jiarong, Yue Xiaodai, et al. Phase Transformation on Chemically Corroded Surface of a Single-Crystal Superalloy During In-Situ Tension at Elevated Temperatures[J]. Rare Metal Materials and Engineering, 2026, 55(03): 595-601. DOI: https://doi.org/10.12442/j.issn.1002-185X.20250094.

ARTICLE

Phase Transformation on Chemically Corroded Surface of a Single-Crystal Superalloy During In-Situ Tension at Elevated Temperatures

Wang Rui, Li Jiarong, Yue Xiaodai, Zhao Jinqian, Yang Wanpeng

Science and Technology on Advanced High Temperature Structural Materials Laboratory, Beijing Institute of Aeronautical Materials, Beijing 100095, China

Abstract: In-situ tensile tests were conducted on a chemically corroded third-generation single-crystal superalloy DD9 at 980 and 1100 ℃. The phase transformation in the surface areas during the tensile process was analyzed using field emission scanning electron microscope, energy dispersive X-ray spectroscope, electron probe X-ray microanalysis, and transmission electron microscope. The phase transformation mechanism on the surface and the influence mechanism were studied through observation and dynamic calculation. During tensile tests at elevated temperatures, chemical corrosion promotes the precipitation of topologically close-packed (tcp) μ phase and σ phase on the alloy surface. Both the precipitation amount and size of these two phases on the surface at 1100 ℃ are greater than those at 980 ℃. The precipitation of tcp phase on the alloy surface results in the formation of an influence layer on the surface area, and the distribution characteristics of alloying elements are significantly different from those of the substrate. The depth of the influence layer at 1100 ℃ is greater than that at 980 ℃. The precipitation of tcp phase prompts the phase transition from γ phase to γ' phase around the tcp phase.

Key words: single-crystal superalloy; in-situ tension; tcp phase; phase transformation; alloying element

1 Introduction

Single-crystal superalloys are critical materials for advanced aircraft engine turbine blades due to their exceptional high-temperature performance[1–4]. Crystal defects, such as stray grains[5–6], freckles[7–8], and low-angle grain boundaries[9], are inevitable to appear during the preparation of single-crystal turbine blades. The crystal defects undermine the crystal integrity of single-crystal turbine blades. Therefore, chemical corrosion is commonly employed to detect these defects. However, chemical corrosion can also alter the surface structure of single-crystal turbine blades, which may affect the microstructure evolution of single-crystal turbine blades under service environments and further affect their performance. Many researchers have conducted research on the effects of chemical corrosion on single-crystal superalloys, mainly including the effects of chemical corrosion on surface morphology, microstructure[10–12], and mechanical properties[13].

Therefore, it is of great significance to research the influence of corrosion on single-crystal superalloys. However, there is little research on the evolution of surface microstructure of single-crystal superalloys after chemical corrosion under high temperature and stress conditions, which is of great importance for the application of single-crystal superalloys. In this research, in-situ tension of a single-crystal superalloy after chemical corrosion was conducted to reveal the phase transformation in the corroded alloy surface during the tensile process at elevated temperatures.

2 Experiment

The material used in this research was the third-generation single-crystal superalloy DD9, and its chemical composition[14] is 3.5wt% Cr, 7.0wt% Co, 2.0wt% Mo, 6.5wt% W, 7.5wt% Ta, 4.5wt% Re, 0.5wt% Nb, 5.6wt% Al, 0.1wt% Hf, 0.008wt% C, 0.001wt% Y, and balanced Ni. Test

Received date: February 26, 2025
Corresponding author: Li Jiarong, Ph. D., Professor, Science and Technology on Advanced High Temperature Structural Materials Laboratory, Beijing Institute of Aeronautical Materials, Beijing 100095, P. R. China, Tel: 0086-10-62497202, E-mail: jrli126@126.com

plates with the length of 100 mm, width of 40 mm, and height of 10 mm were prepared using the seed crystal method. The standard heat treatment (pre-treatment+1340 ℃/6 h/air cooling+1140 ℃/6 h/air cooling+870 ℃/32 h/air cooling) was conducted on the as-cast test plates, and then the samples for in-situ tensile tests (Fig. 1) were taken from the test plates after heat treatment. The samples were ground and polished, followed by chemical etching at 25 ℃ using the reagent of 200 mL H_2O+160 mL HCl+50 g $CuSO_4$+10 mL H_2SO_4. The etching time was 20 s. Afterwards, the samples were rinsed with purified water. After etching, the samples were subjected to in-situ tensile tests at 980 and 1100 ℃ using the Zeiss Sigma300 field emission electron microscope (FESEM). The loading rate for the in-situ tensile test was 20 N/s. Observation and analysis were conducted on the microstructure evolution of the alloy during the tensile process. Dynamic calculations were also applied through JMatPro software.

After in-situ tensile tests, FESEM and energy dispersive X-ray spectroscope (EDS) were used near the fracture surfaces, and the element distribution was characterized through electron probe X-ray microanalysis (EPMA) in a JXA-iHP200F analyzer. The samples for transmission electron microscope (TEM, Tecnai G^2 F20) observation were prepared: a thin slice with a thickness of 0.4 mm was cut from the cross-section of the sample with about 5 mm away from the fracture surface; then, the thin slice was ground until the thickness was less than 50 μm. After that, the thin slice was punched into a disk with a diameter of 3 mm for electrolytic twin-jet through an electrolyte of 10vol% $HClO_4$ ethanol solution.

3 Results

3.1 Initial phase composition

The phase structure of the samples before in-situ tensile test is shown in Fig.2. The initial microstructure shows cuboidal γ' precipitates (approximately 0.342 μm) in γ matrix.

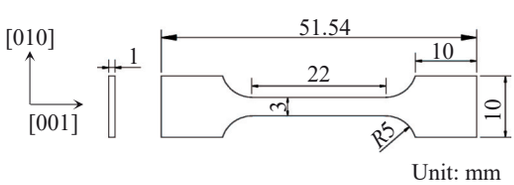

Fig.1 Schematic diagram of in-situ tensile sample

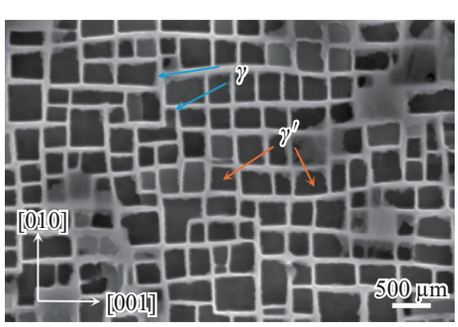

Fig.2 Phase composition of sample before in-situ tensile test

3.2 Phase evolution during in-situ tensile test

Fig.3 shows the phase evolutions during tensile tests at 980 and 1100 ℃. The γ' phase that maintains cubic and dispersed point-like phase can be observed at 267 MPa under the temperature of 980 ℃. As the stress increases to 600 MPa, there is no significant change in the morphology of the γ and γ' phases, and the number and size of the point-like precipitates increase. Numerous white phases are precipitated when the stress reaches 167 MPa under the temperature of 1100 ℃. The precipitates can be divided into two types: spherical-like and needle-like. The number of the spherical- and needle-like precipitates decreases slightly while the size increases when the stress increases to 600 MPa, which conforms to the precipitation growth model of Ostwald Ripening[15]. In addition, the contrast of the γ matrix phase fades obviously. This is due to the element diffusion. Therefore, the number and size of the precipitates at 1100 ℃ are greater than those at 980 ℃. The precipitation of these abovementioned phases on the surface is rarely reported during the tensile tests in other alloys[16].

EDS analyses in Fig. 4 identify these precipitates as topologically close-packed (tcp) phases: the spherical-like μ phase and the needle-like σ phase[17–23].

The sample after the in-situ tensile test at 1100 ℃ is ground slightly, followed by polishing and corrosion for FESEM observations. The resultant microstructure is shown in Fig. 5. The γ' phase still maintains a certain cubic shape, but it is elongated along the direction of tensile stress. The tcp phase cannot be observed, which means no tcp phase precipitation occurs beneath the surface. Therefore, precipitation of tcp phase occurs only on the surface during the tensile process at elevated temperatures.

3.3 Effects of tcp phase precipitation on alloying element distribution

The precipitation of tcp phase in single-crystal superalloys can affect the alloy properties[24–28]. To investigate the effect of the precipitation of tcp phase on the alloy surface, the cross- and longitudinal-sections of the samples after in-situ tensile fracture at 980 and 1100 ℃ were observed and analyzed.

Fig.6a and 6b show the microstructures of the longitudinal-section near the fracture surface of the alloy after in-situ tension at 980 and 1100 ℃, respectively. A certain number of slip bands and micropores can be observed. In Fig. 6a, tcp phase presents as a clustering distribution. It is noteworthy that the γ phase disappears in the clustering areas of tcp phase. Furthermore, micropores tend to form in the areas of tcp phase clusters. However, as shown in Fig.6b, tcp phase is uniformly distributed in the alloy surface rather than in the clusters. The morphologies of the γ/γ' phase cannot be distinguished. The distribution of micropores is not significantly related to the position of the tcp phase.

To analyze the depth of the influence layer resulting from the precipitation of tcp phase on the surface, the cross-sections of samples after in-situ tensile fracture at 980 and

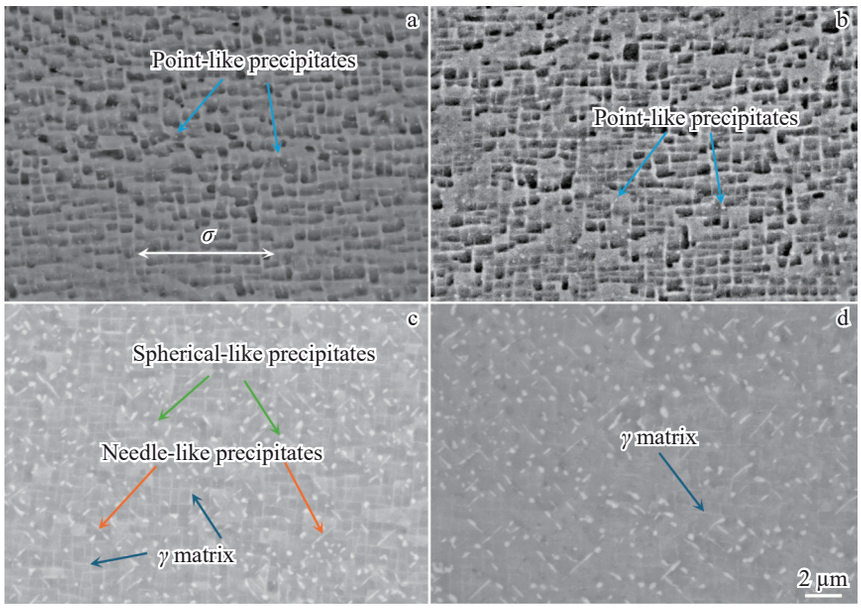

Fig.3 Microstructure evolution of alloy surface during tensile tests under different conditions: (a) 980 ℃/267 MPa; (b) 980 ℃/600 MPa; (c) 1100 ℃/167 MPa; (d) 1100 ℃/600 MPa

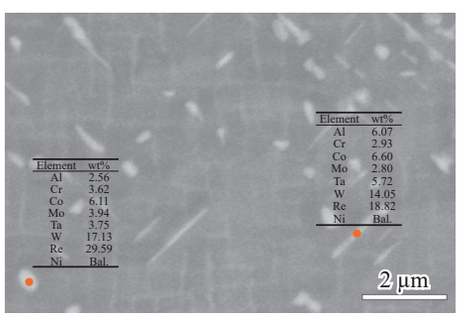

Fig.4 FESEM image and EDS point analyses of spherical-like μ phase and needle-like σ phase

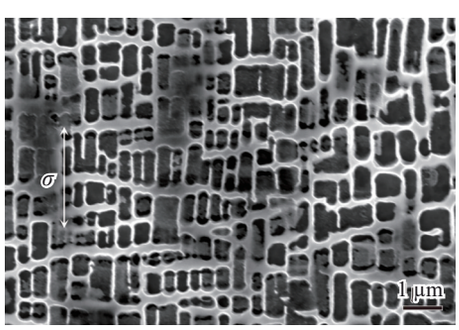

Fig.5 Microstructure beneath sample surface after tensile test at 1100 ℃

1100 ℃ were ground, polished, and observed. The results are shown in Fig.7. There are brighter areas near the surface, and the contrast area at 1100 ℃ (approximately 0.5 μm) is wider than that at 980 ℃ (approximately 0.3 μm), which indicates that the precipitation of tcp phase on the alloy surface causes a larger influence layer on the alloy surface at 1100 ℃. But the thickness of influence layer under both conditions is less than 1 μm. The cross-section of samples after in-situ tensile fracture at 1100 ℃ was selected for further analysis of the effect of abnormal tcp phase precipitation on the alloy.

Fig. 8 shows EDS line scanning analyses of area near alloy surface after in-situ tensile test at 1100 ℃ . There are pronounced distinctions in the element contents of different areas. An irregular layer with different element distributions exists in the surface area of the alloy. Moreover, the distribution characteristics of alloying elements are not completely consistent in the irregular layer. A concentration gradient of alloying elements exists. For example, Re and W contents are decreased with the decrease in depth from the surface, as shown in the green areas in Fig. 8c – 8d. Additionally, the distribution of alloying elements is relatively uniform along the depth direction of the alloy, as shown in the yellow areas in Fig.8c–8d.

4 Discussions

It is indicated that the precipitation of tcp phase occurs on the corroded alloy surface during the in-situ high-temperature tensile process. The precipitation of tcp phase can cause a certain influence on the microstructure of the alloys.

4.1 Precipitation mechanism of tcp phase

The consequence of the corrosion of the alloy surface by the reagents used in this study is that γ' phase dissolves in the reagents and it is corroded, while γ phase remains on the surface, as shown in Fig. 2. Therefore, corrosion results in variations of the chemical composition of the alloy surface. The chemical composition of the polished surface and corroded surface is determined, as shown in Fig. 9a and 9b, respectively. The results demonstrate that the corrosion promotes an increase in content of elements, such as W and Re, on the surface, which is beneficial to the precipitation of

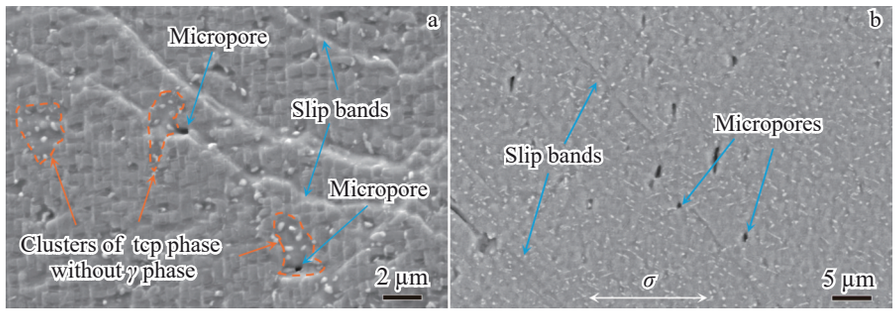

Fig.6 Microstructures of longitudinal-section of alloy surface after in-situ tensile fracture at 980 ℃ (a) and 1100 ℃ (b)

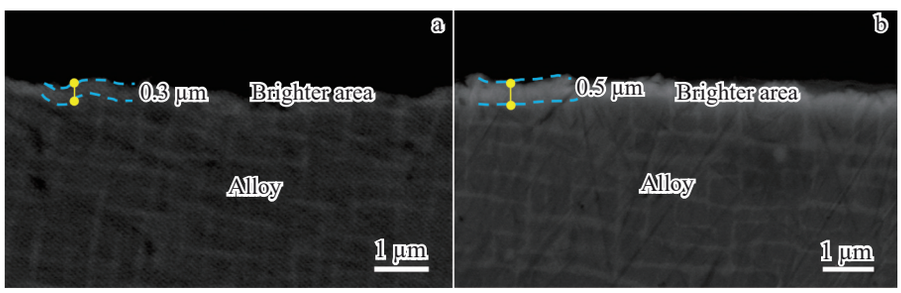

Fig.7 Microstructures of cross-section of alloy surface after in-situ tensile fracture at 980 ℃ (a) and 1100 ℃ (b)

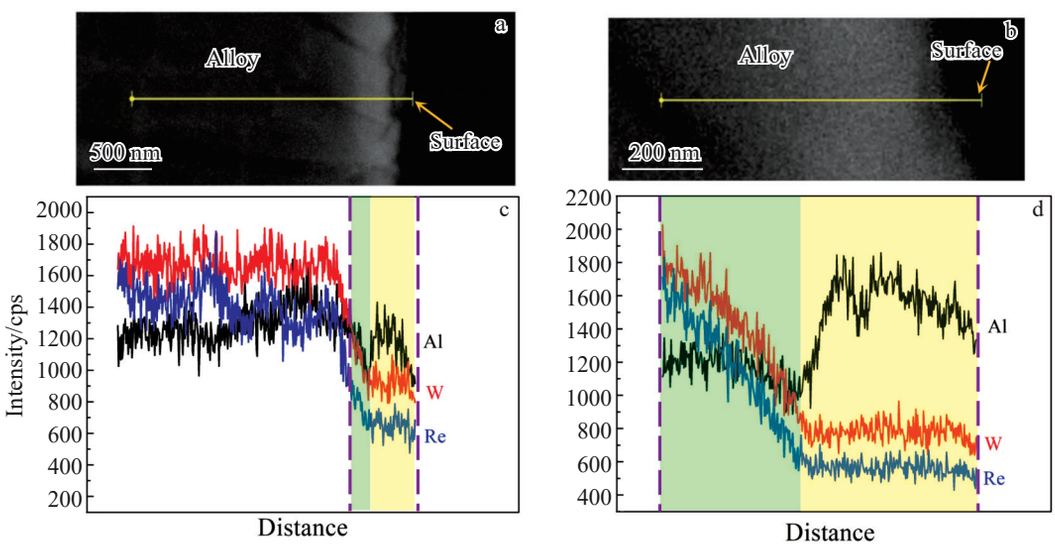

Fig.8 EDS line scanning images (a–b) and analyses (c–d) of area near alloy surface after in-situ tensile test at 1100 ℃: (a, c) low magnification; (b, d) high magnification

tcp phase, according to Fig.4 and the results in Ref.[29–30]. Furthermore, dynamic calculations were performed to analyze the effect of the alteration of chemical composition induced by corrosion on the precipitation of tcp phases, as shown in Fig.9c–9d. It can be seen that 0.5vol% μ phase and σ phase are precipitated in the single-crystal superalloys. Thus, it is concluded that the corrosion on the alloy surface promotes the precipitation of tcp phases.

In addition, the precipitation of tcp phase cannot be observed during the in-situ tensile test of the electrolytically corroded single-crystal superalloy[16]. γ' phase remains on the surface, while γ phase dissolves after electrolytic corrosion[16], which is opposite to the results in this research. Therefore, one reason for the precipitation of tcp phase on the alloy surface during the tensile process at elevated temperature is that the chemical corrosion dissolves the γ' phase, leaving the γ phase in the surface area of the alloy. However, the elements forming tcp phases, such as Re and W, are segregated in the γ phase, triggering an increase in content of elements forming tcp phases, and eventually resulting in the abnormal precipitation of tcp phases on the alloy surface under high temperature and stress conditions.

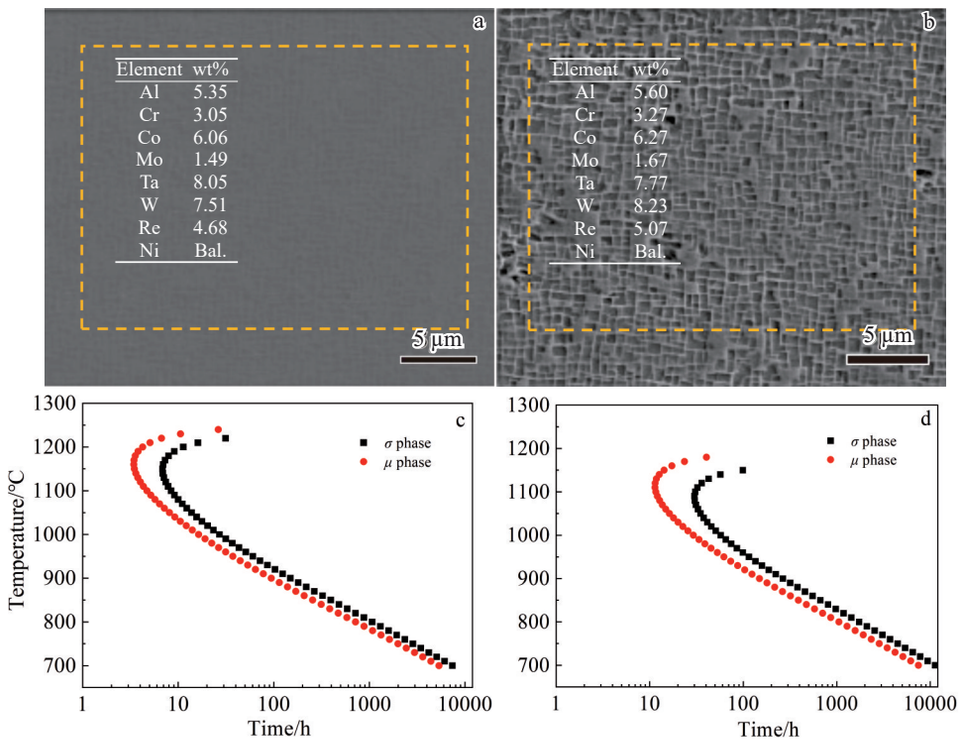

Fig.9 SEM images with EDS analysis results (a–b) and dynamic calculations of tcp phase precipitation (c–d) of polished surface (a, c) and corroded surface (b, d) of samples

4.2 Influence of tcp phase precipitation on alloying element distribution

To investigate the influence of tcp phase precipitation on alloying element distribution, TEM was performed on the samples after in-situ tensile fracture at 1100 ℃, as shown in Fig. 10. It is indicated that the precipitation of tcp phases consumes elements, such as Re and W, and expels γ' phase-forming elements, such as Ni and Al, to the surrounding areas, thereby promoting the formation of γ' phase around the tcp phases. This process may also cause the clusters of tcp phase without γ phase, as shown in Fig. 6a. Furthermore, EPMA analysis was conducted to study the element distribution of the clusters of tcp phase in the sample after tensile test at 980 ℃, as shown in Fig. 11. Fig. 11 demonstrates that the elements, such as Re and W, are enriched in the tcp and γ phases, while the γ' phase and the abnormal areas around tcp phases are enriched with the elements Ni, Al, and Ta. This result is similar to the precipitation mechanism of tcp phases in Ref.[24].

According to the results in Fig. 8, Fig. 10, and Fig. 11, the precipitation of tcp phase on the surface can absorb the tcp phase-forming elements, such as Re and W, from the surface and the regions beneath the surface. The precipitation of tcp phases on the surface results in the depletion of the tcp phase-forming elements, such as Re and W, on the surface, which generates a gap in element concentration between the surface and region beneath the surface. The gap of element concentration brings about element diffusion of the tcp phase-forming elements towards the alloy surface under elevated temperatures[28]. In the meantime, the precipitation of tcp

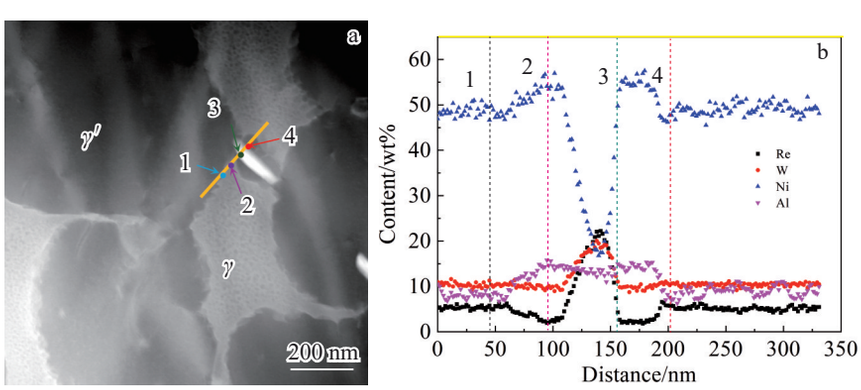

Fig.10 TEM image (a) and corresponding EDS line scanning results (b) of tcp phase in sample after tensile test at 1100 ℃

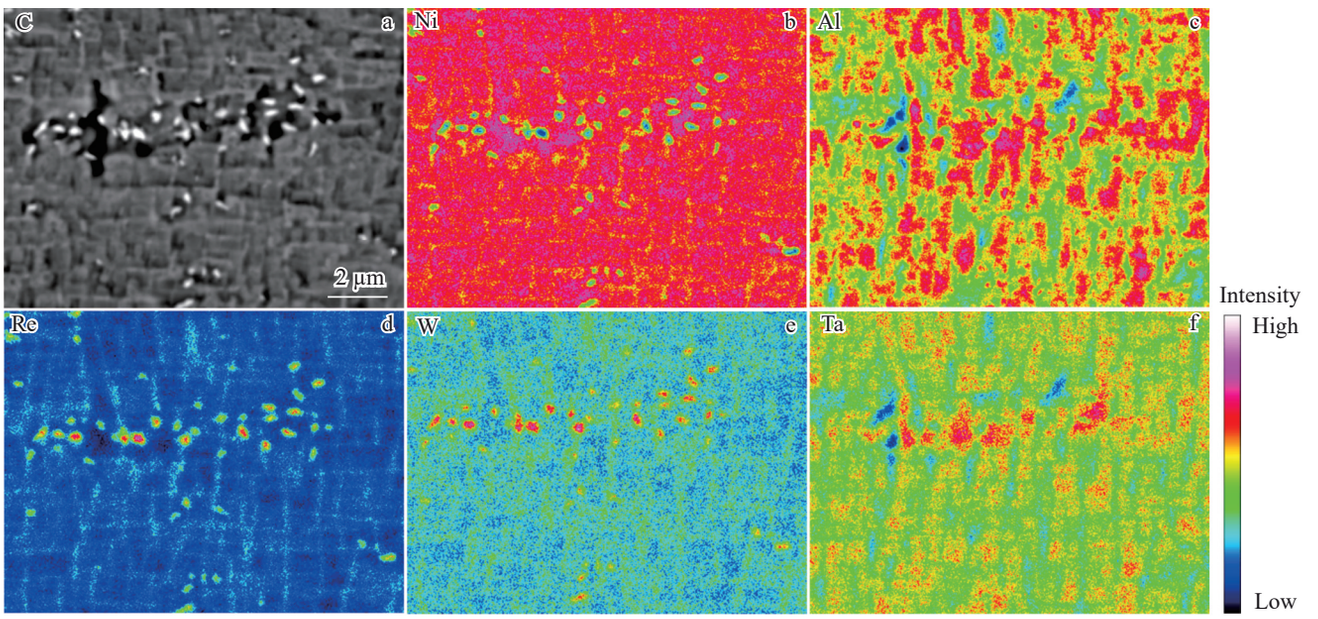

Fig.11 EPMA analysis of alloy after in-situ tensile test at 980 ℃

phases consumes the elements, such as Re and W, giving rise to the phase transformation of γ phase→γ' phase. The growth of tcp phases further consumes the tcp phase-forming elements. The diffusion of alloying elements induced by the phase transition results in the specific characteristics of element distribution, as mentioned in the green and yellow areas in Fig. 8c – 8d. According to Fig. 9, the precipitation tendency of tcp phases in the alloy at 1100 ℃ is greater than that at 980 ℃ . Therefore, the influence layer caused by precipitation of tcp phases at 1100 ℃ is thicker than that at 980 ℃, as shown in Fig.7.

Additionally, the phase transformation of γ phase→γ' phase induced by precipitation of tcp phases causes the formation of the clusters of tcp phase without γ phase, and the γ phase on the alloy surface are hardly observed with the increase in content of tcp phase, as shown in Fig. 3. Furthermore, the elements, such as Re and W, consumed by the precipitation of tcp phases are solid-solution-strengthening elements in the alloy[31]. The precipitation of tcp phases may lead to a decrease in strength of the areas surrounding them. Therefore, micropores are prone to appearance around the tcp phase on the alloy surface during tension at 980 ℃, as shown in Fig.6a. However, the micropores do not exhibit a significant positional tendency during tension at 1100 ℃. This is because numerous tcp phases are dispersedly distributed on the alloy surface without the clusters of tcp phase. Hence, the micropores on the alloy surface display an inconspicuous tendency in position, as shown in Fig.6b.

5 Conclusions

1) Corrosion applied on the single crystal superalloy samples for in-situ tensile tests dissolves γ' phase, while γ phase remains on the surface. The increase in content of elements, such as Re and W, on the surface promotes the tcp phase precipitation, including μ phase and σ phase, on the alloy surface during tensile processes at elevated temperatures.

2) The precipitation of tcp phase in the surface consumes the tcp phase-forming elements, such as Re and W, which prompts the phase transformation from γ phase to γ' phase around the tcp phase, resulting in the disappearance of γ phase during the tensile tests. Furthermore, the precipitation of tcp phase on the alloy surface results in the formation of an influence layer with the thickness less than 1 μm, and the distribution characteristics of alloying elements are significantly different from those of the substrate.

3) The amount and size of the tcp phase precipitated on the surface at 1100 ℃ are greater than those at 980 ℃, leading to a deeper degree of phase transformation from γ phase to γ' phase and a thicker influence layer during the tensile test.

References

1 Celel A D, Duhl D N. *Superalloys 1988*[C]. Seven Springs: The Metallurgical Society, 1988: 235

2 Harris K, Erickson G L, Sikkenga S L *et al*. *Superalloys 1992*[C]. Seven Springs: The Metallurgical Society, 1992: 297

3 Walston W S, Ohara K S, Ross E W *et al*. *Superalloys 1996*[C]. Seven Springs: The Metallurgical Society, 1996: 27

4 Li J R, Zhong Z G, Tang D Z *et al*. *Superalloys 2000*[C]. Seven Springs: The Metallurgical Society, 2000: 777

5 Stanford N, Djakovic A, Shollock B A *et al*. *Scripta Materialia*[J], 2004, 50(1): 159

6 Yang X, Ness D, Lee P D *et al*. *Materials Science and Engineering A*[J], 2005, 413–414: 571

7 Wang Z, Li J R, Liu S Z *et al*. *Journal of Alloys and Compounds*[J], 2022, 981: 165631

8 Ma Dexin. *Acta Metallurgica Sinica*[J], 2016, 52(4): 426 (in

Chinese)
9 Zhao J Q, Li J R, Liu S Z *et al*. *Rare Metal Materials and Engineering*[J], 2007, 36(12): 2232
10 Hu L J, Li J R, Liu S Z *et al*. *Foundry Technology*[J], 2017, 38(3): 525
11 Xue Y P, Hu L J, Zhao J Q *et al*. *Journal of Materials Engineering*[J], 2016, 44(2): 1
12 Song P, Jiang X W, Wu J J *et al*. *Journal of Materials Engineering*[J], 2021, 49(6): 109
13 Dong Jianmin, Li Jiarong, Han Mei. *Journal of Materials Engineering*[J], 2020, 48(1): 77 (in Chinese)
14 Li J R, Liu S Z, Wang X *et al*. *Superalloys 2016*[C]. Seven Springs: The Metallurgical Society, 2016: 57
15 Ratke L, Voorhees P W. *Growth and Coarsening*[M]. Berlin: Springer, 2002
16 Ma Jinyao, Wang Jin, Zhao Yunsong *et al*. *Acta Metallurgical Sinica*[J], 2019, 55(8): 987 (in Chinese)
17 Huo J, Shi Q, Zheng Y *et al*. *Materials Characterization*[J], 2017, 124: 73
18 Lee S, Do J, Jang K *et al*. *Scripta Materialia*[J], 2023, 222: 115041
19 Dubiel B, Indyka P, Moskalewicz T *et al*. *Journal of Microscopy*[J], 2017, 266 (3): 239
20 Cheng Y, Zhao X B, Xia W S *et al*. *Materials & Design*[J], 2024, 237: 112582
21 Li J G, Sun J X, Liu J L *et al*. *Journal of Materials Science & Technology*[J], 2024, 173: 149
22 Gao S, Liu Z Q, Li C F *et al*. *Acta Materialia*[J], 2016, 110: 268
23 Gao S, Liu Z Q, Li C F *et al*. *Journal of Alloys and Compounds*[J], 2014, 610: 589
24 Xia W S, Zhao X B, Yue L *et al*. *Journal of Materials Science & Technology*[J], 2021, 982: 88
25 Cheng K, Jo C, Jin T *et al*. *Journal of Alloys and Compounds*[J], 2011, 509(25): 7078
26 Seiser B, Drautz R, Pettifor D G. *Acta Materialia*[J], 2011, 59(2): 749
27 Shi Q Y, Ding X F, Chen J Y *et al*. *Metallurgical and Materials Transactions A*[J], 2014, 45: 1665
28 Zhao Jie, Ye Fei, Wang Qing. *Fundamentals of Materials Science* [M]. Dalian: Dalian University of Technology Press, 2015 (in Chinese)
29 Cui Jinyan, Zhang Jianting, Yao Jian *et al*. *Rare Metal Materials and Engineering*[J], 2023, 52(4): 1490 (in Chinese)
30 Cheng Yuan, Zhao Xinbao, Yue Quanzhao *et al*. *Rare Metal Materials and Engineering*[J], 2023, 52(7): 2599 (in Chinese)
31 Li Jiarong, Xiong Jichun, Tang Dingzhong. *Advanced High Temperature Structural Materials and Technology*[M]. Beijing: National Defense Industry Press, 2012 (in Chinese)

一种单晶高温合金高温原位拉伸过程中化学腐蚀表面的相转变

王　锐，李嘉荣，岳晓岱，赵金乾，杨万鹏
(北京航空材料研究院 先进高温结构材料重点实验室，北京 100095)

摘　要：对化学腐蚀后的单晶高温合金进行了980和1100 ℃下的原位拉伸试验。使用场发射扫描电子显微镜、能量色散X射线光谱、电子探针X射线显微分析和透射电子显微镜分析了拉伸过程中表面的相变过程。通过观察和动力学计算相结合，研究了合金表面相变机理及其对合金的影响机理。结果表明：在高温拉伸过程中，化学腐蚀促进了合金表面μ相和σ相等拓扑密排（tcp）相的析出。在1100 ℃下，2种相在表面的析出量和尺寸均大于980 ℃下的析出量和尺寸。tcp相在合金表面的析出导致了表面区域1层影响层的形成，该影响层中的合金元素分布特征与合金基体的合金元素分布特征存在明显差异。1100 ℃下形成的影响层厚度大于980 ℃下的影响层厚度。tcp相的析出促使tcp相周围的γ相转变为γ'相。

关键词：单晶高温合金；原位拉伸；tcp相；相转变；合金元素

作者简介：王 锐，男，1994年生，博士生，北京航空材料研究院先进高温结构材料重点实验室，北京 100095，电话：010-62498309，E-mail：WR0608@126.com